Modeling of an implantable device for remote arterial pressure measurement

J. A. Miguel, Y. Lechuga, R. Mozuelos, M. Martinez
Microelectronic Engineering Group, Dept. of Electronics Technology, Systems and Automation Engineering (TEISA), University of Cantabria, Av. Los Castros s/n, Santander, Spain E-39005

ABSTRACT

Cardiovascular diseases are the leading causes of illness and death in Europe, having a major impact on healthcare costs. An intelligent stent (e-stent), capable of obtaining and transmitting measurements of physiological parameters, can be a useful tool for real-time monitorization of arterial blockage without patient hospitalization. In this paper, a behavioral model of a pressure sensing-based e-stent is proposed and simulated under several restenosis conditions. Special attention has been given to the need of an accurate fault model, obtained from realistic finite-element simulations, to ensure long-term reliability; particularly for those faults whose behavior cannot be described by usual analytical models.

Keywords: Biomedical electronics, implantable biomedical devices, biomedical transducers, MEMS testing, Fault Injection, Fault modeling.

1. INTRODUCTION

Cardiovascular diseases (CVD) are the leading cause of morbidity and mortality in the European Union (EU), being responsible for nearly 36% of all deaths in the year 2011[1]. This scenario is expected to worsen due to the progressive ageing of the European population, usually associated with an increasing risk of developing cardiovascular diseases. The high prevalence of these medical conditions contributes considerably to the continuous growth of healthcare burdens, having an immediate impact on its financial sustainability. In 2010, the average healthcare spending of EU member states reached the 9% of their Gross Domestic Product (GDP)[1]. More particularly, diagnosis and treatment of cardiovascular diseases cost the healthcare system nearly 9% of the total healthcare expenditure. The hospitalization of patients suffering from CVD accounted for the 49% of all those cost, while CVD related drug prescriptions accounted for about 29%[2]. Home monitoring systems have been proposed as an interesting alternative to the traditional resource consuming diagnosis techniques. A continuous monitoring of physiological signals related to CVD can provide useful clinical data to cardiologists, used to adapt the medication to the condition of the patient; improving his quality of life, slowing the evolution of the disease and reducing the frequency of hospitalizations.

Nowadays, Percutaneous Coronary Interventions (PCIs) are the most common procedures to restore circulation to patients with narrowed or even blocked arteries. PCI is a less invasive and non-surgical procedure, performed on a sedated but not asleep patient. During the procedure, also known as angioplasty, a balloon catheter is threaded through the blood vessels into the place where the blockage is located. Once the narrowing is reached, the balloon is inflated. The pressure applied by the balloon cracks and compresses the material depositions responsible for the blockage into the vessel walls. The balloon is then deflated and withdrawn, so the blood flow in the vessel is restored. Usually, PCI is combined with the permanent placement of a biocompatible mesh tube called a stent. The stent is placed surrounding the balloon tip and is expanded during its filling. The pressure applied by the inflated balloon locks the stent into place, remaining inside the vessel after the catheter is removed. Stent implantation reduces the risk of elastic recoil and spasms, keeping the vessel open.

Angioplasty with stenting has had a strong impact in modern cardiovascular medicine, positioning as a minimally invasive alternative to coronary artery bypass grafting surgery (CABG), with a short recovery time and similar rate of success. Particularly, the Universitary Hospital Marqués de Valdecilla in Santander (Spain) conducts more than 1500 procedures with stent implantation per year. Unfortunately, this procedure is not exempt of complications comprising its long-term results. In-stent restenosis (ISR) consists of a re-occlusion of a previously treated blood vessel in patients who had undergone an angioplasty procedure with stent implantation. The degree of stress induced to the vessel walls during PCI triggers several physiological repair mechanisms, such as platelet aggregation or neointimal tissue proliferation[3]. In some cases, the growth of tissue inside the stent can be thick enough to reduce the circumference of the lumen in more

Bio-MEMS and Medical Microdevices, edited by Angeliki Tserepi, Manuel Delgado-Restituto, Eleni Makarona
Proc. of SPIE Vol. 8765, 876508 · © 2013 SPIE · CCC code: 1605-7422/13/$18 · doi: 10.1117/12.2017458

than 50%, leading to a restenosis condition. Regular procedures for ISR monitoring include techniques like angiography and echocardiography, which are expensive, time consuming and resource demanding; involving a high impact on national healthcare costs. Moreover, acute ISR conditions can be difficult to fix and can lead to the repetition of the whole angioplasty procedure or even to a bypass surgical intervention. The incidence rate of ISR varies from 10% to more than 70%, regarding the nature of the disease and the type of stent used[3]. The recent introduction of drug-eluting stents, coated with anti-proliferative drugs which are slowly released to the blood flow, has lowered the ISR ratio to nearly 10%, at the expense of higher costs. Despite this improvement, the incidence of restenosis keeps on being an important limitation to PCI.

The fast development of Micro-Electro-Mechanical Systems (MEMS) over the last decade, together with new micro-fabrication technologies compatible with CMOS fabrication processes, have made possible the integration of sensor structures and electronic circuits in the same chip. In this way, it has been possible to highly increase the capabilities and potential uses of implantable medical electronic devices. An intelligent stent (e-stent) capable of sensing and transmitting real-time measurements of physiological parameters related to blood vessel occlusion, such as pressure and flow velocity, can be a useful tool to ISR early detection and follow-up without patient hospitalization[4 5 6].

It is relevant to point out that an implantable device for ISR monitoring must match certain design restrictions, including reduced size, low power consumption, reasonable cost, output stability and above all, high reliability over extended periods without the need for recalibration. This is why heterogeneous testing, fault modelling and fault injection are critical issues to validate the fabricated device. One of the objectives of this work focuses on the generation of fault models for implantable capacitive MEMS pressure sensors, usually used to measure blood flow pressure in implanted devices. This will be a first step towards the development of a comprehensive MEMS testing methodology.

In this paper a behavioural model of an ISR monitoring device is described and evaluated under different grades of stenosis. Special attention has been given to the analysis of MEMS pressure sensors, in order to estimate the influence of their most common fabrication faults on the system response. In Section 2 three blood flow measurement techniques, reported to be compatible with intelligent stent design, are described and compared. Section 3 describes the behavioural model of the proposed implantable device under different grades of stenosis, in order to validate its response under real ISR conditions. In Section 4 analytical models of a MEMS pressure sensor are presented and validated using FEM simulations. A reported fabrication fault error is injected into the FEM model, so that its influence on the sensor response can be quantified. The paper finishes in Section 5 with the conclusions and future work.

2. BLOOD FLOW MEASUREMENT TECHNIQUES

Blood flow measurement is one of the most usual techniques for monitoring various types of cardiovascular diseases. Its value is routinely collected in hospitals using invasive nonimplantable sensors, usually requiring catheterization. Several measurement techniques have been recently reported to be compatible with intelligent stent design, in order to develop a reliable device for implantable blood flow sensing in patients who had undergone PCI with stent implantation. The most promising measurement approaches are based on electromagnetic, ultrasonic and pressure-measurement techniques. These three techniques will be described in detail along this chapter, and their specific advantages and disadvantages will be considered.

2.1 Electromagnetic

Intelligent stents with electromagnetic flow measurement capabilities are based on a direct application of Hall-effect. This effect is produced when an electrically conductive fluid passes through a magnetic field. Then, the magnetic field exerts a transverse force on the charge carriers in the flow, creating a voltage difference, which is perpendicular to the flow and to the magnetic field itself. A couple of electrodes are responsible for measuring the balancing electric potential. The magnitude of the voltage measured by these two diametrically opposed electrodes attached to the vessel walls[7], is given by,

$$V_{EM} = D \cdot B \cdot v \cdot \cos\varphi \cdot \cos\theta \,. \tag{1}$$

Where D is the diameter of the blood vessel, B is the magnetic flux density and v is the blood flow cross-sectional mean velocity. The angles θ and φ, represents the magnetic field alignment with the flow and the generated electric field.

Nonimplantable electromagnetic flow meters are designed to setup a magnetic field perpendicular to the blood flow direction, in order to maximize the accuracy of the measurement. As can be seen in (1), this technique presents a strong

dependence upon the magnetic field alignment with the blood vessel, making the measurement highly sensitive to the position of the magnetic field source. This magnetic source can be internally or externally applied. The former approach requires a surgical intervention to implant the source near the blood vessel. It provides an accurate alignment between the blood flow direction and the magnetic field, at the expense of highly increasing the costs of the procedure. The latter approach is based on an external application of the magnetic field; it does not imply surgery and causes no discomfort to the patient. Its main disadvantage remains the lack of accuracy in the positioning of the source, leading to a degradation of the velocity measurement. Besides, the implanted sensing electrodes must be placed diametrically opposed to guarantee the reliability of the measurement. A shift between the actual placement of the electrodes and the desired diametrical line, due to a non-uniform expansion of the angioplasty balloon, also produces significant deviations in blood flow measurements. In both cases, an efficient correction method will be needed to ensure the precision of the measurements[4], raising the complexity and cost of the device.

2.2 Ultrasound

Ultrasound flow measurement techniques use the principles of Doppler shift. The frequency change between an emitted sound wave and the received one is proportional to the relative velocity between the sound source and the observer. In the particular case of blood flow meters, Doppler systems are based on the analysis of frequency shifts in ultrasound signals scattered from red blood cells[7]. These frequency shifts are related to the velocity of blood particles through the following expression,

$$\Delta f = \frac{2 \cdot v \cdot f_T}{c} \cdot \cos\theta \,. \tag{2}$$

Where v is the blood flow velocity, c is the propagation velocity of the sound waves through human body tissues, Δf is the Doppler frequency shift, f_T is the transmitted sound wave frequency and θ is the angle between the axis of the emitted sound wave and the direction of the blood flow.

Doppler effect is the basis for thoracic and esophageal echocardiogram, commonly used nowadays in hospital procedures. However, the adaptation of this technique to implantable devices must overcome some drawbacks before being completely reliable. First, as can be seen in (2), the flow measurement is highly sensitive to the location of the sound transducer. Second, the sound wave generation may need a significant amount of power, which would make necessary the use of an implanted battery. Third, the complexity in processing the received signal may need bulky and power demanding electronics.

The frequency of the emitted pulse must be thoroughly selected to reach the inner parts of the body without compromising the resolution of the measurement. Low frequency ultrasound waves present high tissue penetration and low resolution, while high frequency ultrasonic waves have a better resolution but are only able to scan the surface of the tissue. This is why external ultrasound Doppler blood-flow meters are incapable to reach deep inside patient's body without sacrificing the degree of resolution in the measurements.

Devices bringing the ultrasound transmitter and receiver closer to the blood vessel can avoid the previous limitations, using an ultrasound frequency high enough to allow good resolution[5]. However, it is necessary to overcome important physical constraints to make this device implantable. Among them we can highlight the alignment issues between the probe and the vessel and the amount of energy needed to generate the ultrasound waveform.

2.3 Pressure

Blood flow velocity in a clogged or narrowed vessel can be stated as a function of the pressure gradient between both sides of the blockage[8]. The general expression can be written as,

$$\Delta P = R_1 \cdot v + R_2 \cdot v^2 + R_3 \cdot \frac{dv}{dt} \,. \tag{3}$$

Where ΔP is the pressure gradient between distal and proximal sides of the stent, v is the mean cross-sectional flow velocity in the vessel and R_1, R_2 and R_3 are coefficients that depend on fluid properties and the geometry of the obstruction. R_1 represents losses due to fluid viscosity and it is directly related to the length of the stenosis. R_2 represents nonlinear losses due to the flow difference between downstream and upstream locations and it is determined by the relationship between the transversal un-stented area of the obstructed vessel and its total area. R_3 is related to fluid inertial effects, and can be neglected under circumstances of medium to severe stenosis[8].

Pressure-based techniques seem to be the most promising ones for several reasons. First, the possibility of using simple MEM structures as transducers allows the integration of sensors and electronics in the same silicon substrate, decreasing the cost and size of the system. The low energy requirement of capacitive pressure sensors, when compared to piezo-resistive alternatives, makes possible to reduce the size of the device; since its powering can be carried out wirelessly using inductive coupling techniques. Moreover, this measurement approach obtains readings of the absolute pressure inside the blood vessel, providing a complete set of data for its clinical consultation.

An intelligent stent based on pressure measurement techniques for ISR monitoring presents the simplest possible implementation. A device of this kind just comprises a pair of capacitive MEMS pressure sensors placed at opposed sides of the stent, and an inductance to form a resonant LC tank used to transmit the collected data to an external reader via inductive coupling[4]. Figure 1 shows a simplified model of an intelligent stent for ISR follow-up based on pressure sensing techniques, emphasizing on sensor placement inside the blood vessel. The parameter P_0 is the proximal pressure measured in the heart side of the stent, while P_1 is the distal pressure sensed at the opposite end of the stent. More complex devices incorporate electronic circuits to process the data acquired by the sensors within the Integrated Circuit (IC) itself, in order to improve the performance of the system[6].

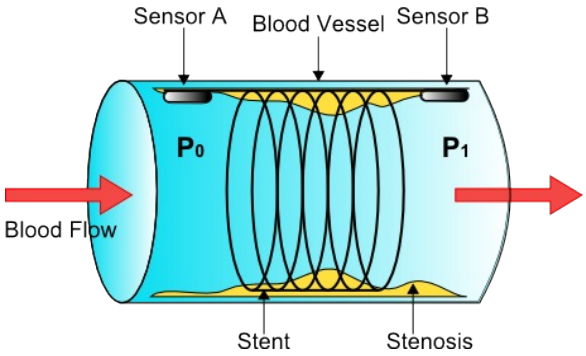

Figure 1. Schematic view of an intelligent stent for ISR monitoring, based on pressure-measurement techniques.

3. ELECTRONIC SYSTEM

Prior to the design of the intelligent stent, it is necessary to determine the place where the device is going to be implanted. In this way, the design constraints will be adjusted to the particular operation conditions expected at the location of interest. Pulmonary artery has been selected to be the vessel to treat with the proposed intelligent stent. Supravalvar Pulmonary Artery Stenosis (SPAS) is a congenital defect that produces an undesired narrowing of the pulmonary artery, the large blood vessel that conducts blood form the right ventricle of the heart to the lungs. The narrowing of this artery will force the heart to increase the pumping strength to maintain the regular blood flow, leading to an enlarged heart and to high blood pressure in the right side of the heart. A significant increase in right ventricular systolic pressure may result in a possible failure of the heart.

Congenital SPAS is a condition that exists at birth, and can occur either in isolation or accompanied with other congenital heart defects. Its most common treatment choice comprises an angioplasty procedure with stent implantation; with the exception of those cases where the narrowing of the artery is so thick that an angioplasty repair is not effective. In that case, corrective surgery may be required, followed by stent implantation to treat post-surgical lesions. Balloon expandable stents can be implanted in small infants as a bridge to later surgical interventions in the pulmonary artery, adding the advantage that they can be easily redilated as the children grows or in the case of restenosis occurrence. For this reason, an intelligent stent can be implanted in a stenosed pulmonary artery without altering its treatment course, providing useful information to detect and monitor the evolution of restenosis, as well as to select the most appropriate time to conduct a new dilation of the stent.

A simplified model of an implantable device for arterial blood flow measurement in the pulmonary artery, based on pressure sensing, is described throughout this section. The behavioral model of the proposed intelligent stent has been divided into 3 consecutive blocks, as shown in Figure 2. Each one of these blocks has been described using the mathematical simulation tool Matlab. In order to perform a general validation of the model under real restenosis conditions, different levels of occlusion have been simulated by varying the blockage parameters R_1 and R_2 according to data sets obtained from medical reports[9].

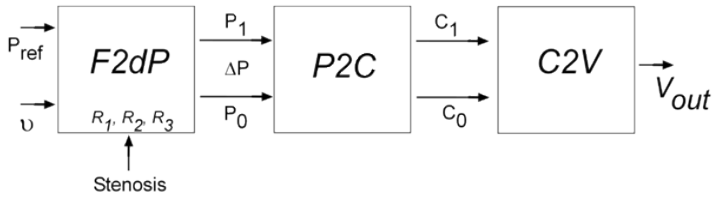

Figure 2. Simplified model of the electronic system divided into three blocks: Frequency-to-Pressure block (F2dP), Pressure-to-Capacitance block (P2C) and Capacitance-to-Voltage block (C2V).

The first block of the model, F2dP in Figure 2, describes the relationship between blood flow velocity in a stenosed vessel and blood pressure gradient along the blockage, through the geometrical parameters of the obstruction R_1 and R_2, as expressed in (3). This block presents three inputs, labeled as P_{ref}, υ and *Stenosis*. Input P_{ref} corresponds to a pressure signal from a branch pulmonary artery, and υ is the blood flow velocity signal from the same blood vessel. The third input, noted as *Stenosis*, reflects blockage parameters R_1 and R_2, which can be varied to simulate different grades of restenosis in the artery. The set of values for R_1 and R_2, as seen in Table 1, has been collected from medical research publications relating blood flow velocity and pressure gradient in a clogged coronary artery[9]. These values have been estimated using an indirect procedure, by applying equation (3) to measured blood flow velocity and pressure signals in arteries with different occlusions. However, stenosis shape can also be estimated using direct measurement techniques, such as angiographies and intravascular ultrasonographies.

Table 1. Characteristics of the relationship between instantaneous blood flow velocity and pressure gradient in a stenosed blood vessel.

	R_1	**R_2**
Normal artery	0.032 ± 0.018	0.00030 ± 0.0049
Intermediate stenosis	0.15 ± 0.11	0.0021 ± 0.0014
Severe stenosis	2.67 ± 1.58	0.0014 ± 0.010

Using the above mentioned inputs, the F2dP block generates two output pressure signals: P_0 and P_1. These signals correspond to the pressure waveforms to be acquired by the sensors placed at distal and proximal sides of the stent. Signal P_0 will be measured by the sensor placed at the heart-side of the stent, while P_1 will be measured by the one located at the opposite end of the device. It must be noticed that signals P_0 and P_1 are generated for a particular grade of occlusion in the artery, specified by the values of parameters R_1 and R_2. Figure 3 (a) shows the blood flow and pressure signals from a healthy pulmonary artery, while Figure 3 (b) shows the output signals generated by the F2dP block, P_0 and P_1, for a clinical condition of low stenosis rate.

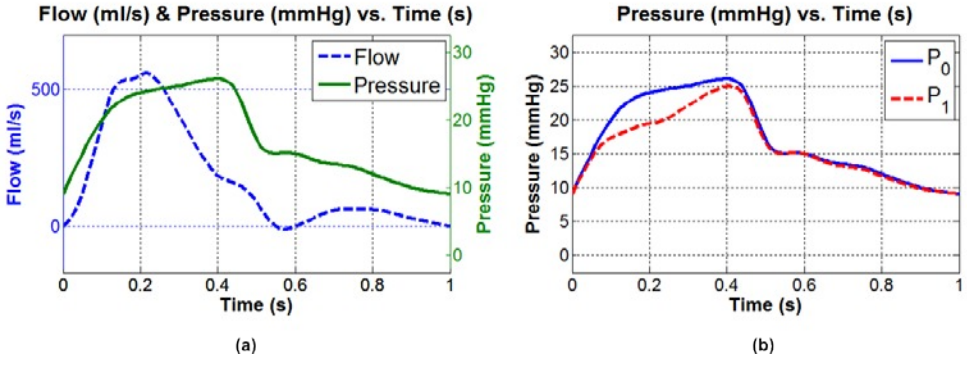

Figure 3. Relation of input and output signals from F2dP block: (a) Pressure and flow signals of a healthy pulmonary artery obtained from clinical trials, (b) distal and proximal pressure signals generated by the first block of the model.

The second block of the model, called P2C, describes analytically the behavior of a capacitive MEMS pressure sensor. The principle of operation of this kind of sensors is similar to that of parallel plate capacitors, where the equivalent capacitance is proportional to the area of two conductive plates and inversely proportional to their separation. The physical structure of these sensors comprises a fully clamped diaphragm suspended at a certain distance over a fixed backplate. Once a uniformly distributed pressure is applied to the sensor, the flexible diaphragm deforms towards the fixed backplate until the elastic force balances the pressure, reducing the initial gap between both plates, and increasing the resultant capacitance.

As mentioned, the P2C block uses analytical expressions to fully describe the response of the pressure sensors. The relationship between capacitance and pressure of the actual sensor included in the model is shown in Figure 3 (a). It can be seen that its sensing pressure range has been selected to fit values bellow the maximum pressure related to a condition of moderate stenosis in the pulmonary artery, which corresponds to a measure of 60 mmHg. During section 4 will be seen that this assumption can be considered to be true for almost ideal sensors, where their behavior can be accurately modeled using mathematical expressions. In the case of capacitive MEMS pressure sensors with injected fabrication faults, it won't be possible to easily adjust their behavior to analytical expressions; so the use of Finite Element Analysis (FEA) tools will be necessary to characterize the influence of the faults on their response.

The last block of the model, C2V, performs the conversion of the capacitive output signals from the pressure sensors into digital voltage signals. These electric signals reflect the absolute pressure measurements collected by the sensors, and their difference can be used to calculate the pressure gradient between opposite ends of the stents.

As exposed in (3), the output voltage signals from the C2V block, together with a slight knowledge of the obstruction parameters R_1 and R_2, provide enough information to accurately estimate blood flow velocity in a vessel. The capacitance-to-voltage converter (CVC) modeled in block C2V has been selected to match the characteristics of the most commonly used capacitance-to-digital converters (CDC)[10]. The response of the proposed C2V block can be seen in Figure 4 (b).

The modeled CDC presents the following properties: a reference capacitance of 1.5 pF, a conversion range of 1.7 pF, and a resolution of 10 bits, selected to maintain the power requirements of the converter as low as possible without compromising the resolution of the measurements. Moreover, several undesired effects, usually observed in real converters, such as gain error, capacitive input noise, absolute error after calibration, integral non-linearity and differential non-linearity, have been considered to analyze their influence in the response of the system. The values of the aforementioned parameters have been selected to be similar to their typical magnitudes, in order to obtain a first approximation of their influence over the accuracy in the estimation of the blood flow velocity.

In this way, it is possible to obtain a first approximation to the response of the whole electronic system. The behavior of the modeled system for a low ISR condition in a branch pulmonary artery, defined by the parameters R_1=0.032 and R_2=0.0003, is shown in Figure 5. The reference blood flow waveform is represented, together with the difference of the output voltage signals of the system. As can be seen, both traces are highly correlated, allowing an accurate estimation of blood flow in the artery based on the analysis of the generated output voltage.

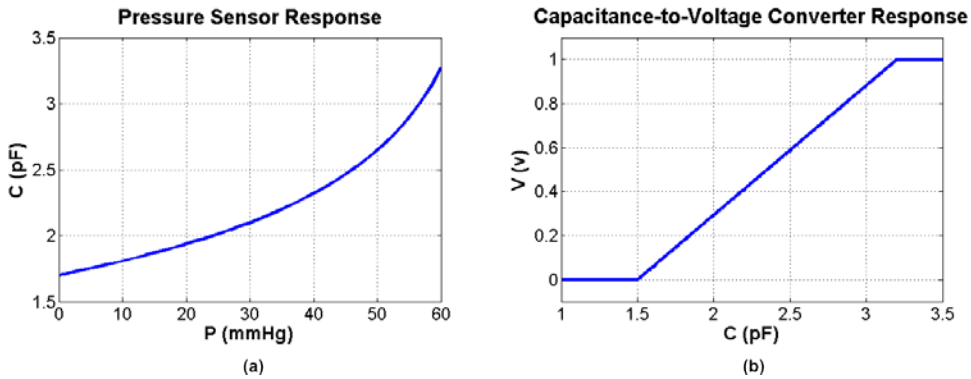

Figure 4. Analytical models of blocks P2C and C2V: (a) Capacitive MEMS pressure sensor response, (b) Capacitance-to-Digital converter response.

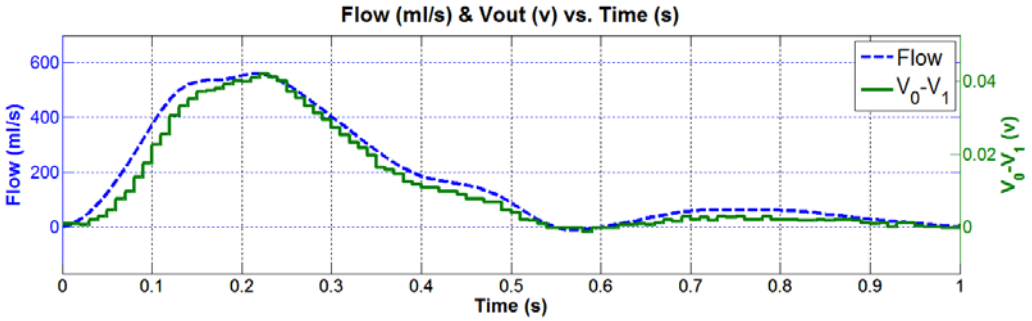

Figure 5. Output voltage difference from C2V block, compared to the reference blood flow signal to be estimated.

This behavioral model also allows displaying the output mean voltage when different ISR conditions are considered, by introducing several sets of R_1 and R_2 parameters. In this way, the model has been tested for restenosis grades between none and moderate, proving to generate reliable results for every medical condition analyzed. As can be seen in Figure 6, worse grades of blockage in the artery, reflected in higher R_1 and R_2 values, produce an increment in the pressure gradient along the stent; raising the mean output voltage of the system, as expected from (3). These results have been compared with experimental data collected from clinical trials[11], showing similar behavior.

It must be considered that the previous analyses have been carried out using a fault-free analytical model of the MEMS pressure sensor. As will be seen in the next section, this mathematical model of the sensor cannot be applied under the presence of certain fabrication faults. In that case, new behavioral models of the sensor must be obtained from FEA tools and included into the P2C block, in order to evaluate its influence in the response of the whole system.

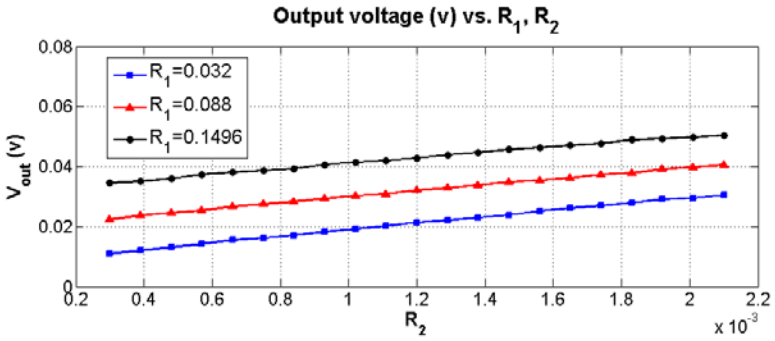

Figure 6. Output mean value of the system for a sweep of R_1 and R_2 parameters, corresponding to grades of none, mild and moderate stenosis in the pulmonary artery.

4. CAPACITIVE MEMS PRESSURE SENSOR

4.1 Fault-free sensor

The operation basis of a capacitive MEMS pressure sensor is similar to that of a parallel plate capacitor, as mentioned in section 3. Figure 7 presents a simplified cross-sectional view of a sensor of this kind, based on a flexible top diaphragm suspended at a certain distance over a fixed backplate; where P is the uniformly distributed pressure applied to the diaphragm, w_0 is the deflection of the diaphragm center, t_g is the separation between the plates when the pressure applied to the sensor and the one in the cavity are equal, and t_m is the thickness of the diaphragm.

The deflection of a fully clamped circular thin diaphragm, with a thickness-to-radius ratio lower than 1/10, can be analytically expressed as a function of the distance from the center of the plate[12]. Several assumptions must be considered to validate this analytical expression: (a) diaphragm material must have isotropic mechanical properties, (b) the metallic electrodes located on top of the plates must be thinner than the plates themselves to be neglected, (c) the undeflected gap between both plates must be small compared to lateral extents of the plates, so that the electric field fringing effect can be despicable, (d) the residual stresses in the flexible diaphragm are not considered.

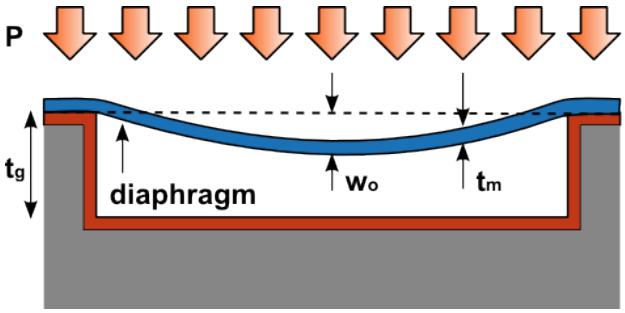

Figure 7. Cross sectional view of a capacitive MEMS pressure sensor, under the effect of a uniformly distributed pressure

Once fulfilled the previous requirements, the relationship between the deflection of a fully-clamped circular diaphragm and the radial distance to its center, can be stated as:

$$w(r) = w_0 \cdot \left[1 - \left(\frac{r}{a}\right)^2\right]^2 . \tag{4}$$

Where r is the distance between the point of interest and the center of the diaphragm, a is the radius of the diaphragm and w_0 is the maximum center deflection.

The center deflection of a diaphragm can be calculated using different analytical expressions, depending on the relationship between its maximum deflection and the thickness of the diaphragm[12]. A flexible diaphragm can be considered a plate under small deflection conditions when its maximum deformation is less or equal than 30% of its thickness. In this case, the center deflection of the diaphragm can be noted as a linear function of the applied pressure, via the following equation:

$$w_0 = \frac{3 \cdot P \cdot a^4 \cdot \left(1 - \mu^2\right)}{16 \cdot E \cdot t_m^3} . \tag{5}$$

Where μ and E are the Poisson's ratio and the Young's elasticity modulus of the diaphragm material, respectively.

On the other hand, a flexible diaphragm with a maximum deformation beyond 30% of its thickness is considered a plate under conditions of large deflection. Then, the relationship between the center deflection of the plate and the applied pressure can be analytically stated by a non-linear function:

$$w_0 = \frac{3 \cdot P \cdot a^4 \cdot \left(1 - \mu^2\right)}{16 \cdot E \cdot t_m^3} \cdot \frac{1}{1 + \dfrac{0.488 \cdot w_0^2}{t_m^2}} . \tag{6}$$

It can be noticed that, in the case of small deflections $w_0 << t_m$, equations (6) and (5) can be approximated. Figure 8 shows the center deformation of a thin diaphragm under conditions of both small and large deflection. The results from equations (5) and (6) present short differences for the case of $w_0 < 0.03 \cdot t_m$. For this reason, equation (6) has been used to model the behavior of the sensor in both deflection circumstances. All of the results shown in this section have been obtained from a reference sensor based on a polysilicon (E=169 GPa, υ=0.22) diaphragm of 4 µm thick, with a radius of 350 µm and a sealed cavity of 2 µm height.

The equivalent capacitance of a pressure sensor, based on a thin diaphragm, can be analytically calculated as a function of its radial deflection by:

$$\Delta C = C_S - C_0 = \iint_A \frac{\varepsilon_0 \cdot dA}{t_g - w(r)} - \varepsilon_0 \cdot \frac{A}{t_g} . \tag{7}$$

Where C_0 is the capacitance of the sensor when no pressure difference exists between the cavity and the outside environment, ε_0 is the dielectric permittivity of free space and A is the area of the plates.

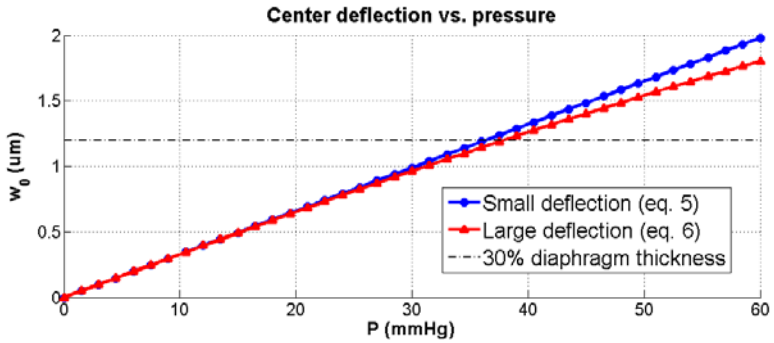

Figure 8. Comparison of diaphragm center deflection vs. pressure, under small and large deflection conditions.

Replacing *w(r)* by (4) in the expression (7) it is possible to obtain a direct relationship between the capacitance of the sensor and the pressure difference between the sealed cavity and the external environment:

$$C = \frac{\varepsilon_0 \cdot A}{t_g} \cdot \sqrt{\frac{t_g}{w_0}} \cdot \tanh^{-1}\left(\sqrt{\frac{w_0}{t_g}}\right) = C_0 \cdot \sqrt{\frac{t_g}{w_0}} \cdot \tanh^{-1}\left(\sqrt{\frac{w_0}{t_g}}\right). \quad (8)$$

Finite Element Analysis techniques allow non-linear multi-domain simulations of complex 3D structures. In the case of MEMS pressure sensors, using FEA tools it is possible to calculate both the deflection and the capacitance of a sensor structure when a particular uniformly distributed pressure is applied. Thus, FEA results enable the validation of the above mentioned analytical models under different environmental conditions, as well as calculating the response of the sensor when a particular fabrication defect is injected in its structural model. Figure 9 shows a comparison between deflection and capacitance results obtained from analytical models and FEA computational tools. A behavioral model of the diaphragm has been developed using equations (4), (6) and (8) under a Matlab simulation environment. In the same way, a finite element model of the sensor has been built using the FEA tool Ansys. According to the results obtained, analytical-based models provide an acceptable estimation of the behavior of our reference sensor in a fault-free scenario.

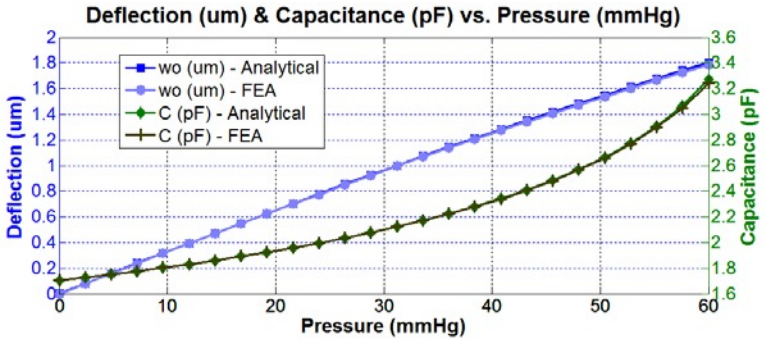

Figure 9. Comparison of center deflection and equivalent capacitance results for a reference sensor simulated using analytical models and FEA tools.

4.2 FE fault injection

Among the most important requirements for every implantable biomedical device, high reliability over an extended period of time should be highlighted. For this reason, device testing and fault modeling can be considered critical factors for a successful implementation of this kind of systems. This section is focused on fault model generation for a MEMS capacitive pressure sensor, to be included in the implantable device presented in section 3. This model intends to be a first step towards the development of a comprehensive MEMS testing methodology.

Cost-effective manufacturing processes have been a determinant factor for MEMS success. Future advances in this field must include a testing strategy which ensures high quality and reliable devices without strongly increasing its manufacturing costs. This is especially important in safety-critical systems, such as implantable devices, where MEMS play a crucial part in its effective operation.

The impact of fabrication defects on micromechanical structures must be explicitly covered by MEMS fault models. The approach presented in this paper centers on the analysis of faulty behaviors through finite elements simulations of MEMS with injected fabrication defects; particularly for those faults whose behavior cannot be easily described by analytical models.

In the course of MEMS fabrication procedure, failure mechanisms or defects can arise during the CMOS process and the micromachining process[13 14 15]. Over the CMOS process, microelectronic and micromechanical components are fabricated, by means of a set of semiconductor, conductor and dielectric layers. These layers are growth through technological operations, such as oxidation, deposition, photolithography, etching, ion implantation, etc. Each one of them is a potential source of defects, leading to the appearance of harmful residuals to the succeeding step. During the micromachining process, MEMS suspended structures are released by the removal of a sacrificial layer. The post-processing operation to remove this layer, called anisotropic etching, depends on several parameters to be accurately performed, such as etching time, etching rate, adequate chemical solutions, etc. Slight changes in these parameters can lead to a partial release of the structure and/or to the presence of impurities.

Failure mechanisms due to fabrication defects can be classified according to the MEMS compound which has been affected: the physical-electrical interface (gauge), or the microstructure that suspends the gauge. Moreover, each group of faults is in turn grouped in two classes: catastrophic faults, which prevent any utilization of the system; and parametric faults, which alter the microsystem performance by changing the geometry or material parameters of the structure.

For example, anisotropic wet etching of a single silicon crystal is usually performed to release the flexible plate of a MEMS capacitive pressure sensor. During this process, impurities, in the form of small crystal lattice defects, can appear. These defects have been reported to raise pyramids on top of the diaphragm, changing its geometrical characteristics[16]. The sidewall slope of the pyramids is a fixed parameter, determined by the angles between the main crystal planes of a single crystal silicon (54.7º, the angle between a {100} and a {111} plane in case of anisotropic etching of a {100} oriented wafer). As the height of the pyramid is calculated from the sidewall slope, a variation in the base length of the pyramid will alter its size[16 17].

A behavioral model for the deflection of a diaphragm in the presence of pyramids has been developed using FEA tools. A FE model of the diaphragm has been built in Ansys, comprising a circular-shaped thin plate fully clamped on all edges, neglecting any movement or rotation at these points (restricted in all degrees of freedom). Figure10 shows an example of a diaphragm with a pyramid of 20 µm base length located at its center, under an applied pressure of 60 mmHg.

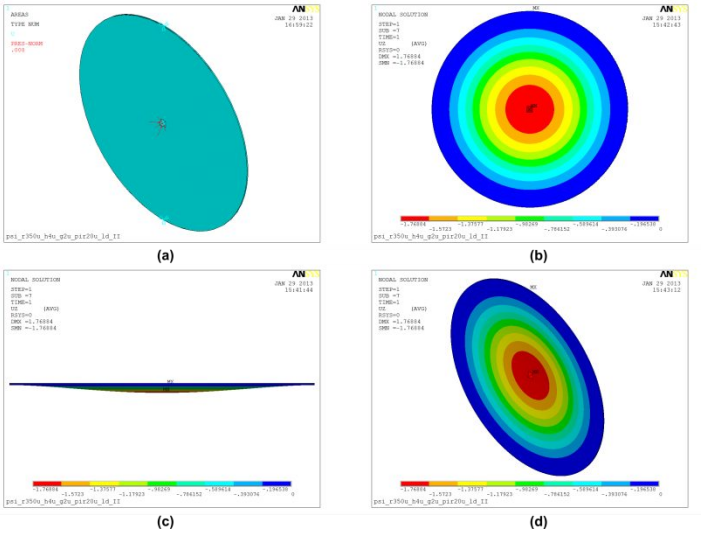

Figure 10. Screenshot of diaphragm with a pyramid (base=400 µm^2) at its center under a pressure of 8 kPa: (a) Structural model in Ansys; (b) top, (c) lateral and (d) isometric views of deflection results.

Pyramids on the diaphragm have been modeled to have: (a) different base areas on the same centered position of the diaphragm; and (b) the same size but different locations along the radius of the plate. Figure 11 (b) shows the capacitance results for our reference sensor, under a constant pressure of 60 mmHg, with pyramids of base areas up to

2500 µm^2, located at the center of the plate. As can be noticed, the influence of a pyramid is proportional to its size. Bigger pyramids significantly reduce the deflection and output capacitance of the sensor, implying a sensitivity loss which can seriously compromise its reliability.

In the same way, Figure 11 (b) contains the output capacitance results for the same sensor, calculated for different locations of a pyramid with a base side of 50 µm. As can be observed, the maximum sensitivity loss is obtained for pyramids placed at the center and sides of the diaphragm. In a fault-free case, the center and anchoring locations of the diaphragm present maximum bending conditions. The presence of a rigid object, like a solid pyramid, prevents any bending of the plate at its location. Hence, the influence of these defects will be stronger when found at the center and sides of the plate, as evidenced in Figure 11 (b).

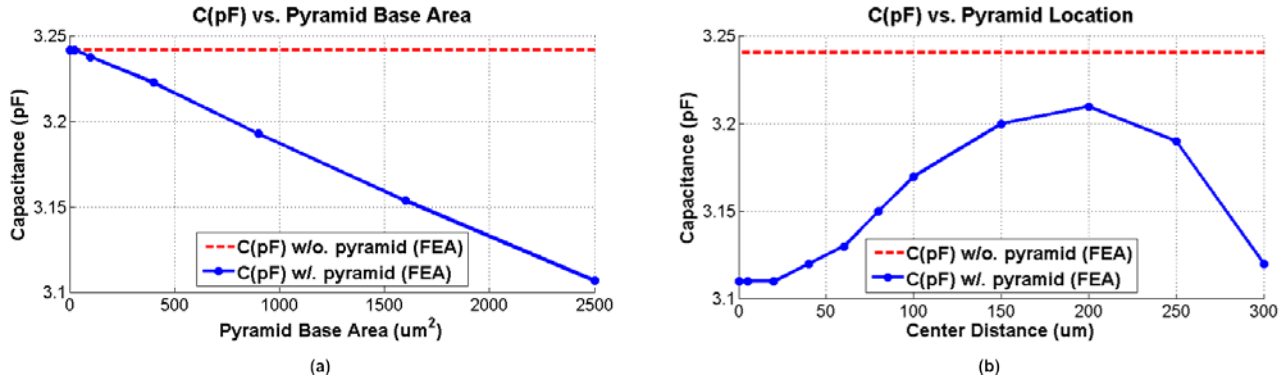

Figure 11. (a) Sensor capacitance for different pyramid base sizes; (b) sensor capacitance for different pyramid locations along the radius of the plate, under a pressure of 60 mmHg.

As shown in Figure 9, the behavior of a MEMS capacitive pressure sensor can be accurately modeled using analytical expression in a fault-free scenario. However, this mathematical formulation is no longer valid for modeling diaphragms with certain fabrication defects. Thus, it is mandatory to create additional sensor models under these faulty conditions, considering deflection and capacitance results obtained from FEA simulations; especially for those defects in which the geometry and/or the material properties of the flexible plate are altered.

5. CONCLUSIONS

Over the past few decades, advances in MEMS fabrication processes, together with the possibility of integrating MEMS sensors and CMOS electronics on the same silicon substrate, have increased the general interest in heterogeneous systems. The development of implantable heterogeneous systems to detect and monitor certain cardiovascular diseases, as an alternative to the costly and resources demanding traditional diagnosis procedures, can help to reduce the total healthcare expenditure in the EU.

In this work, the behavioral model of an implantable intelligent stent for pulmonary artery blood flow sensing has been introduced. Blood flow monitoring devices based on pressure sensors present some interesting advantages when compared with the rest of methodologies analyzed; such as dual blood flow and pressure sensing capabilities, improved robustness and high reliability over extended periods of use. The proposed model has been tested under different grades of restenosis, by varying the geometrical parameters of the occlusion between ranges collected from medial trials; in order to obtain a first approximation of the device behavior under real disease conditions.

Test-related problems for a capacitive MEMS pressure sensor (based on a circular polysilicon diaphragm of 4 µm thick, with a radius of 350 µm and a sealed cavity of 2 µm height) have been considered through the second half of this work, particularly those cases in which the geometry or the material properties of the diaphragm have been altered. An analytical model has proved to accurately reflect the deflection and capacitance of a fully clamped circular thin plate under fault-free conditions. However, the aforementioned mathematical model evidences a lack of precision when tested under faulty conditions. Therefore, the development of realistic fault models, based on FEA results for flexible diaphragms with injected fabrication faults, seems to be a necessary requirement to fully characterize implantable intelligent stents.

REFERENCES

[1] OECD, [Health at a Glance: Europe 2012], OECD Publishing (2012), http://www.oecd-ilibrary.org/social-issues-migration-health/health-at-a-glance-europe-2012_9789264183896-en.

[2] Nichols M., Townsend N., Luengo-Fernandez R., Leal J., Gray A., Scarborough P. and Rayner M., [European Cardiovascular Disease Statistics 2012], European Heart Network, Brussels, European Society of Cardiology, Sophia Antipolis (2012).

[3] Hoffmann, R. and Mintz, G.S., "Coronary in-stent restenosis - predictors, treatment and prevention," European Heart Journal 21, 1739-1749 (2000).

[4] Takahata, K., Gianchandani, Y. B. and Wise, K.D., "Micromachined Antenna Stents and Cuffs for Monitoring Intraluminal Pressure and Flow," Journal of Microelectromechanical Systems 15(5), 1289-1298 (2006).

[5] Wang, M. and Chen, J., "Volumetric Flow Measurement Using an Implantable CMUT Array," IEEE Transactions on Biomedical Circuits and Systems 5(3), 214-222 (2011).

[6] Chow, E.Y., Chlebowski, A.L., Chakraborty, S., Chappell, W.J. and Irazoqui, P.P., "Fully Wireless Implantable Cardiovascular Pressure Monitor Integrated with a Medical Stent," IEEE Transactions on Biomedical Engineering 57(6), 1487-1496 (2010).

[7] Webster, J.G., [The Measurement, Instrumentation and Sensors Handbook], CRC Press, Boca Raton, FL(1999).

[8] Young, D.F., "Some factors affecting pressure-flow relationships for arterial stenoses," ASME Conf. Appl. Mech. Bioeng. Flu. Eng., 87-90, 1983.

[9] Marques, K.M.J., [Combined flow and pressure measurements in coronary artery disease], Vrije Universiteit, Amsterdam (2008).

[10] Arfah, N., Alam, A.H.M.Z. and Khan, S., "Capacitance-to-voltage converter for capacitance measuring system," 4th International Conference on Mechatronics, 1-4 (2011).

[11] Rothman, A., Perry, S.B., Keane, J.F. and Lock, J.E., "Early results and follow-up of balloon angioplasty for branch pulmonary artery stenoses," Journal of the American College of Cardiology 15(5), 1109-1117 (1990).

[12] Timoshenko, S., [Theory of Plates and Shells], McGraw-Hill, New York (1940).

[13] Castillejo, A., Veychard, D., Mir, S., Karam, J. and Courtois, B., "Failure Mechanisms and Fault Classes for CMOS-Compatible Microelectromechanical Systems," IEEE International Test Conference, 541-550 (1998).

[14] Mir, S., Charlot, B. and Courtois, B., "Extending Fault-Based Testing to Microelectromechanical Systems," Journal of Electronic Testing: Theory and Applications 16, 279-288 (2000).

[15] Huang, Y., Vasan, A.S.S., Doraiswami, R., Osterman, M. and Pecht, M., "MEMS Reliability Review," IEEE Transactions on Device and Materials Reliability 12(2), 482-493 (2012).

[16] Landsberger, L. M., Nashed, S., Kahrizi, M. and Paranjape, M., "On Hillocks Generated During Anisotropic Etching of Si in TMAH," Journal of Microelectromechanical Systems 5(2), 106-116 (1996).

[17] Rosing, R., Reichenbach, R. and Richardson, A., "Generation of component level fault models for MEMS," Microelectronics Journal 33, 861-868 (2002).